THE JOURNAL OF BIOLOGICAL CHEMISTRY VOL. 288, NO. 50, pp. 35637–35650, December 13, 2013

The HECT Type Ubiquitin Ligase NEDL2 Is Degraded by Anaphase-promoting Complex/Cyclosome (APC/C)-Cdh1, and Its Tight Regulation Maintains the Metaphase to Anaphase Transition*[S]

Received for publication, March 23, 2013, and in revised form, October 24, 2013 Published, JBC Papers in Press, October 25, 2013, DOI 10.1074/jbc.M113.472076

Li Lu[‡§], Shaohua Hu[¶], Rongfei Wei[‡‖], Xiao Qiu[‡‖], Kefeng Lu[‡], Yesheng Fu[‡], Hongchang Li[‡], Guichun Xing[‡], Dong Li[‡], Ruiyun Peng[¶], Fuchu He[‡§‖1], and Lingqiang Zhang[‡2]**

*From the [‡]State Key Laboratory of Proteomics, Beijing Proteome Research Center, Beijing Institute of Radiation Medicine, Beijing 100850, China, the **Institute of Cancer Stem Cells, Dalian Medical University, Dalian, Liaoning Province 116023, China, the [§]College of Life Science and Bio-Engineering, Beijing University of Technology, Beijing 100124, China, the [¶]Department of Experimental Pathology, Beijing Institute of Radiation Medicine, Beijing 100850, China, and the [‖]Department of Biological Sciences and Biotechnology, Tsinghua University, Beijing 100084, China*

Background: NEDL2 is a member of the HECT type ubiquitin ligase NEDD4 family, but its function remains largely unknown.
Results: NEDL2 is degraded by APC/C-Cdh1 during mitotic exit and regulates metaphase to anaphase transition.
Conclusion: NEDL2 appears to dynamically modulate regulation of mitosis.
Significance: Our data provide a novel substrate of APC/C-Cdh1 and reveal an additional protein by which HECT type ubiquitin ligase can regulate mitosis.

NEDD4-like ubiquitin ligase 2 (NEDL2) is a HECT type ubiquitin ligase. NEDL2 enhances p73 transcriptional activity and degrades ATR kinase in lamin misexpressed cells. Compared with the important functions of other HECT type ubiquitin ligase, there is less study concerning the function and regulation of NEDL2. Using primary antibody immunoprecipitation and mass spectrometry, we identify a list of potential proteins that are putative NEDL2-interacting proteins. The candidate list contains many of mitotic proteins, especially including several subunits of anaphase-promoting complex/cyclosome (APC/C) and Cdh1, an activator of APC/C. Cdh1 can interact with NEDL2 *in vivo* and *in vitro*. Cdh1 recognizes one of the NEDL2 destruction boxes ($R^{740}GSL^{743}$) and targets it for degradation in an APC/C-dependent manner during mitotic exit. Overexpression of Cdh1 reduces the protein level of NEDL2, whereas knockdown of Cdh1 increases the protein level of NEDL2 but has no effect on the NEDL2 mRNA level. NEDL2 associates with mitotic spindles, and its protein level reaches a maximum in mitosis. The function of NEDL2 during mitosis is essential because NEDL2 depletion prolongs metaphase, and overexpression of NEDL2 induces chromosomal lagging. Elevated expression of NEDL2 protein and mRNA are both found in colon cancer and cervix cancer. We conclude that NEDL2 is a novel substrate of APC/C-Cdh1 as cells exit mitosis and functions as a regulator of the metaphase to anaphase transition. Its overexpression may contribute to tumorigenesis.

Ubiquitin-mediated proteasomal degradation represents the most critical pathway to control the stability and quality of cellular proteins in eukaryotes. Ubiquitin ligases are responsible for substrate recognition and are divided into two major classes: the RING (really interesting new gene) finger type and HECT (homologous to E6AP carboxyl terminus) domain type ligases (1). The anaphase-promoting complex/cyclosome (APC/C),[3] a RING finger type ubiquitin ligase, is a key ubiquitin ligase that controls several transitions in the cell cycle (2, 3). The activity of the APC/C is tightly regulated in the cell cycle. One of the main regulatory mechanisms for the APC/C is through its association with accessory-activating factors, cell division cycle protein 20 (Cdc20/fizzy) and fizzy/cell division cycle 20-related 1 (Cdh1/Fzr1) (4, 5). Cdc20 associates with the APC/C from prometaphase to anaphase, whereas Cdh1 recognizes mitotic cyclins and additional substrates containing either a destruction box (D-box), composed of the sequence R*XX*L, or the KEN box for degradation in mitotic exit and G_1 phase (6–8).

Among HECT type ligases, there are nine members in the Nedd4 (neural precursor cell-expressed developmentally down-regulated gene 4) family, all of which share a similar structure, including a C2 domain at the N terminus, 2–4 WW domains in the middle of the protein, and a HECT domain at the C terminus (9). Despite being similar in structure, each of the nine NEDD4 family members exhibits unique functions.

* This work was supported by National Basic Research Programs 2012CB910304, 2011CB910602, and 2011CB910802 and National Natural Science Foundation Projects 31125010 and 81221004.
[S] This article contains supplemental Tables S1 and S2 and Movies S1 and S2.
[1] To whom correspondence may be addressed: Beijing Institute of Radiation Medicine, 27 Taiping Rd., Beijing 100850, China. Tel./Fax: 8610-80705115; E-mail: hefc@nic.bmi.ac.cn.
[2] To whom correspondence may be addressed: Beijing Institute of Radiation Medicine, 27 Taiping Rd., Beijing 100850, China. Tel./Fax: 8610-68177417; E-mail: zhanglq@nic.bmi.ac.cn.

[3] The abbreviations used are: APC/C, anaphase-promoting complex/cyclosome; ANAPC, anaphase-promoting complex subunit; IGF, insulin-like growth factor; TRITC, tetramethylrhodamine isothiocyanate; IP, immunoprecipitation; SAC, spindle assembly checkpoint.

Except for NEDD4-like ubiquitin ligase 1 (NEDL1) and NEDD4-like ubiquitin ligase 2 (NEDL2), also known as HECW1 and HECW2, the other seven members can regulate ubiquitin-mediated intracellular trafficking, proteasomal degradation, and nuclear translocation of multiple proteins. They have been found to be involved in many important signaling pathways, such as TGFβ-, EGF-, IGF-, VEGF-, and TNFα-mediated pathways (10). NEDL1 shares large homology with NEDL2. NEDL1 mRNA preferentially expresses in neuronal tissue and highly expresses in neuroblastomas with favorable prognosis (11). NEDL1 is proposed to ubiquitylate mutant SOD1 (superoxide dismutase 1) but not wild-type SOD1, which is found in patients with familial amyotrophic lateral sclerosis. It is thus suggested that mutant SOD1, Dvl1 (dishevelled-1), and TRAP-δ (translocon-associated protein-δ) accumulate as a ubiquitylated complex in neurons, potentially leading to neuronal death (11). Studies in cell lines suggest that NEDL1 stimulates p53-mediated apoptosis (12). Motor neuron degeneration and muscular atrophy occur in the NEDL1 transgenic mouse (13). NEDL2 regulates the stability of p73 (14) and is involved in the degradation of ATR kinase in lamin misexpressed cells (15). Compared with NEDL1 and the other seven members, little is known about NEDL2, and it will be interesting to explore it.

In this study, we first revealed that NEDL2 was localized specifically on mitotic spindles and that its protein level reached a maximum in mitosis and was degraded by APC/C-Cdh1 in a D-box dependent manner during mitotic exit. Moreover, NEDL2 depletion caused a marked delay of the metaphase-anaphase transition, and the overexpression of wild type or mutant NEDL2 containing the C2 domain caused earlier activation of APC/C, leading to chromosome lagging, which may induce tumorigenesis.

EXPERIMENTAL PROCEDURES

Cell Culture and Transfection—HEK293T cells, HeLa cells, and HeLa/GFP-H2B cells were cultured in DMEM supplemented with 10% fetal bovine serum (FBS). Cells were transfected with Lipofectamine 2000 following the manufacturer's protocol (Invitrogen).

Antibody and Reagents—The proteasome inhibitors MG132, nocodazole, taxol, thymidine, and polyclonal antibody NEDL2 were purchased from Sigma-Aldrich. Anti-GAPDH, anti-Cdh1, anti-APC2, and secondary antibodies were purchased from Santa Cruz Biotechnology, Inc. Antibody against Cdc27 was purchased from BD Biosciences. Antibodies against α-tubulin, APC11, Cdc16, or Cdc23 were purchased from Abcam. Anti-HA was from Roche Applied Science. Anti-Myc and anti-FLAG antibodies were from MBL.

Immunoprecipitation and Immunoblotting—For general cell lysis, transfected cells were harvested and lysed in HEPES lysis buffer (20 mM HEPES, pH 7.2, 50 mM NaCl, 0.5% Triton X-100, 1 mM NaF, 1 mM dithiothreitol) and boiled with 2× SDS-PAGE loading buffer. For immunoprecipitation, cell lysates were prepared in 500 ml of HEPES buffer supplemented with protease inhibitor mixture (Roche Applied Science). Immunoprecipitation was performed using mouse anti-FLAG (2.5 mg) for 4 h at 4 °C followed by incubation with protein A/G-agarose beads (Santa Cruz Biotechnology) overnight at 4 °C. Beads were then washed three times in HEPES lysis buffer and examined by immunoblotting with the indicated primary antibodies and appropriate secondary antibody, followed by detection with the Super Signal chemiluminescence kit (Pierce).

SDS-PAGE and Mass Spectrometry—Immunoprecipitates were resolved on 12% Novex Tris/glycine gels. Gels were minimally stained with Coomassie Brilliant Blue to differentiate IgG bands. Each lane was then cut into three molecular weight regions. These bands were digested with 100 ng of trypsin overnight. LTQ Orbitrap Velos (Thermo Fisher Scientific) was run in a data-dependent mode, where each sample was eluted in a 1-h 5–30% acetonitrile gradient. Spectral data were then searched against the human protein RefSeq database in Proteome Discoverer1.3 Suites with Mascot software.

RNA Interference—The NEDL2 siRNA-1 (5′-GUGGGUACCUCCAGUUUAATT-3′), siRNA-2 (5′-CAGGGAAGUUAAAGUUAAUTT-3′), siRNA-3 (5′-GGAGGCCUGAUCAUGUUUATT-3′), Cdh1 siRNA-1 (5′-GAAGGGTCTGTTCACGTATTCCCTT-3′), siRNA-2 (5′-GCAACGATGTGTCTCCCTATT-3′), and non-targeting siRNAs (5′-UUCUCCGAACGUGUCACGU-3′) were synthesized by Shanghai GenePharm. All siRNAs were transfected into the cells according to the manufacturer's protocol.

Immunofluorescence—For subcellular localization analyses, cells were fixed with 4% paraformaldehyde and permeabilized in 0.2% Triton X-100 (PBS). Proteins were stained using the indicated antibodies and detected with a TRITC-conjugated or FITC-conjugated secondary antibody. The nuclei were stained with DAPI (Sigma), and images were visualized with a Zeiss LSM 510 Meta inverted confocal microscope.

In Vitro Degradation and Ubiquitination Assays—For *in vitro* degradation assays, extracts from HeLa cells were prepared. Then, extract was supplemented with degradation mixture (1.5 mg/ml ubiquitin, 7.5 mM creatine phosphate, 1 mM ATP, 1 mM $MgCl_2$, 0.1 mg/ml cycloheximide) and ^{35}S-labeled substrate at 30 °C. Aliquots were removed at the indicated times and resolved by SDS-PAGE and autoradiography. For *in vitro* ubiquitination, G_1 extracts from HeLa cells were immunoprecipitated with anti-Cdc27 antibody-protein A beads for 2 h at 4 °C to purify APC/C. Ubiquitination reactions were initiated by mixing purified APC/C beads with ^{35}S-labeled *in vitro* translated substrate, E1 (50 μg/ml), E2 (50 μg/ml), ubiquitin (1.25 mg/ml), and an energy regeneration mix. Samples from each time point were then analyzed by SDS-PAGE and autoradiography.

Cell Synchronization and Time Lapse Imaging—For double-thymidine arrest, cells were incubated in thymidine-containing (2 mM) medium for 18 h, released into fresh medium for 8 h, and incubated in thymidine-containing (2 mM) medium for 24 h. For thymidine-nocodazole arrest, cells were incubated in thymidine-containing (2 mM) medium for 18 h, released into fresh medium for 3 h, and treated with 100 ng/ml nocodazole for 11 h. G_1/S border cells were obtained by releasing cells synchronized by double-thymidine block into fresh medium for 0 h, whereas S phase and G_2 phase were collected at 4 and 8 h. For mitotic cells, cells were synchronized by thymidine-nocodazole arrest and shaken off. For G_1 cells, nocodazole-arrested cells

TABLE 1

Mitotic proteins identified by mass spectrometry

The functional specificity of the interacting proteins of NEDL2 in HEK293T cells identified by mass spectrometry in supplemental Tables S1 and S2 was further analyzed. Mitotic proteins were chosen from high confidence interactions, both identified in two IP/MS experiments.

Proteins	Description	Other aliases	Accession number
ANAPC1	Anaphase-promoting complex subunit 1	APC1	gi12056971
ANAPC2	Anaphase-promoting complex subunit 2	APC2	gi7019327
CDC27	Cell division cycle protein 27 homolog	APC3	gi167466175
ANAPC4	Anaphase-promoting complex subunit 4	APC4	gi41327749
ANAPC5	Anaphase-promoting complex subunit 5	APC5	gi20127553
CDC16	Cell division cycle protein 16 homolog	APC6	gi118402578
ANAPC7	Anaphase-promoting complex subunit 7	APC7	gi212549738
CDC23	Cell division cycle protein 23 homolog	APC8	gi118402596
FZR1	Fizzy/cell division cycle 20 related 1	CDH1	gi209969680
PRC1	Protein regulator of cytokinesis 1	ASE1	gi40807445
PLK1	Polo-like kinase 1	STPK13	gi21359873
NUSAP1	Nucleolar and spindle-associated protein 1	NUSAP	gi17505234
CENPF	Centromere protein F	CENF	gi55770834
CEP170	Centrosomal protein of 170 kDa	KAB	gi109255232
CLAPS2	Cytoplasmic linker-associated protein 2		gi57863301

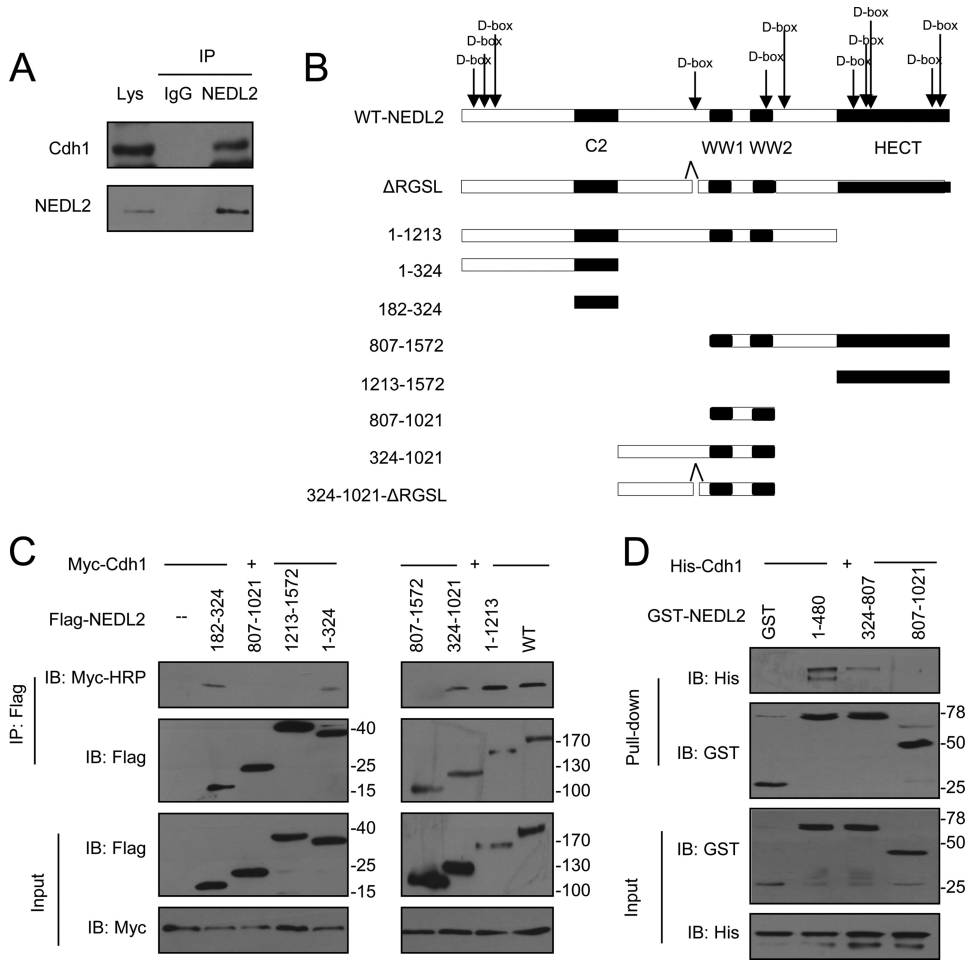

FIGURE 1. **NEDL2 interacts with Cdh1 *in vivo* and *in vitro*.** *A*, co-immunoprecipitation of endogenous NEDL2 and Cdh1 is shown. HeLa cell lysates were prepared and subjected to immunoprecipitation with NEDL2 antibody or IgG and analyzed by immunoblotting using NEDL2 or Cdh1 antibodies. *B*, schematic of a series of NEDL2 deletion mutants; the positions of D-boxes are *labeled*. *C*, NEDL2 deletion mutants and Myc-Cdh1 were transfected into HEK293T cells. Cell lysates were immunoprecipitated with anti-FLAG antibody. Both the lysate and immunoprecipitates were analyzed by immunoblotting (*IB*). *D*, direct interaction between NEDL2 and Cdh1 is revealed by GST pull-down assays. Input and pull-down samples were both subjected to immunoblotting with anti-GST and anti-His antibodies. Input represents 10% of that used for pull-down.

were released into fresh medium for 4 h. Cell cycle distributions were confirmed by flow cytometry.

For time-lapse imaging, HeLa/GFP-H2B stable cell lines were seeded in an eight-chambered cover glass (Lab-Tek Chambered 1.0 Borosilicate Cover Glass System, Nunc). Images were collected every 5 min using a 0.1-s exposure for 12 h using a ×40 (or ×20) lens objective on an inverted fluorescence microscope (Nikon Eclipse Ti-E) with an Ultra View spinning disc confocal scanner unit (PerkinElmer Life Sciences). The temperature of the imaging medium was kept at

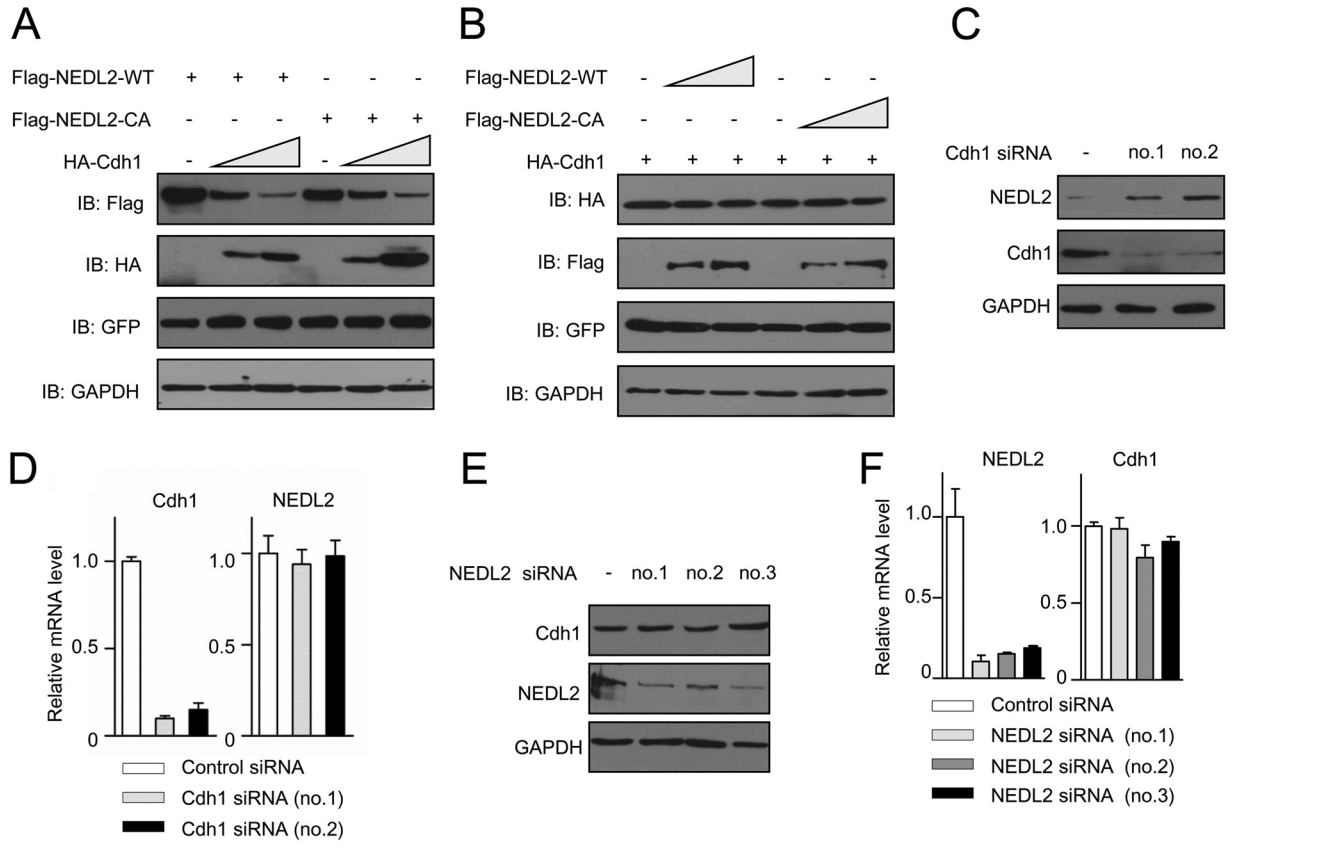
A
Flag-NEDL2-WT + + + - - -
Flag-NEDL2-CA - - - + + +
HA-Cdh1 - - -
IB: Flag
IB: HA
IB: GFP
IB: GAPDH
B
Flag-NEDL2-WT - - - -
Flag-NEDL2-CA - - - -
HA-Cdh1 + + + + + +
IB: HA
IB: Flag
IB: GFP
IB: GAPDH
C
Cdh1 siRNA - no.1 no.2
NEDL2
Cdh1
GAPDH
D
Cdh1
NEDL2
Relative mRNA level
1.0
0.5
0
Control siRNA
Cdh1 siRNA (no.1)
Cdh1 siRNA (no.2)
E
NEDL2 siRNA - no.1 no.2 no.3
Cdh1
NEDL2
GAPDH
F
NEDL2
Cdh1
Relative mRNA level
Control siRNA
NEDL2 siRNA (no.1)
NEDL2 siRNA (no.2)
NEDL2 siRNA (no.3)
G
C-box
Fizzy
Domain
WD40 Repeats
Cdh1
ΔC-box
ΔFizzy
H
Myc-Cdh1 - WT ΔC-box ΔFizzy
Flag-NEDL2 + + + +
IB: Flag
IB: Myc
IB: GFP
IB: GAPDH
I
Myc-Cdh1 - WT ΔC-box ΔFizzy
IB: Cyclin B
IB: Myc
IB: GAPDH
J
Flag-NEDL2 WT 1-324 324-1021 807-1572
HA-Cdh1 - + - + - + - +
IB: Flag
IB: HA
IB: GFP
IB: GAPDH
K
HA-Cdh1 -
Flag-NEDL (2324-1021) + + +
IB: Flag
IB: HA
B: GFP
IB: GAPDH
L
Human eelgevwqrrgslegaaaaa
Mouse gelgevwqrrgslegaaaaa
Rat gelgevwqrrgslegaaaaa
M
Flag-NEDL2 (324-1021) WT ΔRGSL
HA-Cdh1 - + - +
IB: Flag
IB: HA
IB: GFP
IB: GAPDH
N
Flag-NEDL2 WT ΔRGSL
HA-Cdh1 - + - +
IB: Flag
IB: HA
IB: GFP
IB: GAPDH

37 °C. Image sequences were viewed using Volocity software, and cell behavior was analyzed manually.

Real-time RT-PCR—Total RNA was isolated from the cells or tissues using TRIzol (Invitrogen) and reverse-transcribed using 1 μg of total RNA with an oligo(dT) primer. The following primers were used for real-time PCR: human GAPDH forward, 5′-GGGAAGGTGAAGGTCGGAGT-3′; GAPDH reverse, 5′-TTGAGGTCAATGAAGGGGTCA-3′; human NEDL2 forward, 5′-CCAGAGTTCTTCACCGTGCT-3′; NEDL2 reverse, 5′-CCACAAAGAATGCCTTGCCC-3′; human Cdh1 forward, 5′-CAGTGTATCGACACGGGCTC-3′; and Cdh1 reverse, 5′-CACAGACACAGACTCCCACT-3′.

Tissue Array and Immunohistochemistry—The normal tissues and tumor specimens used in tissue microarray (TMA) studies, two serial samples used in testing correlation between NEDL2 and Cdh1 expression, and samples used in analysis of NEDL2 mRNA level were obtained from a tissue bank maintained at Zhongshan Hospital, Fudan University. Approval for this study was obtained from the Zhongshan Hospital Research Ethics Committee. Informed consent was obtained from all subjects or their relatives. After screening hematoxylin and eosin-stained slides for optimal tumor content, we constructed tissue microarray slides (Shanghai Biochip Company, Ltd., Shanghai, China). Two cores of tissue were collected from non-necrotic areas of tumor foci and from peritumoral tissue adjacent to the tumor. The tissue arrays include a microarray including 19 types of normal tissues, a multiple-tumor tissue microarray, a colon tumor tissue microarray, and a cervix tumor tissue microarray containing cancer and matched adjacent normal tissue.

Immunohistochemistry staining for NEDL2 or Cdh1 was carried out on the paraffin-embedded tissue, followed by secondary antibody and 3,3′-diaminobenzadine disclosure and microscopic imaging and analysis. Nuclei were counterstained with hematoxylin. Images were captured using a Nano Zoomer Digital Pathology system (Hamamatsu). The widely accepted German semiquantitative scoring system, considering the staining intensity and area extent, was used. Each specimen was assigned a score according to the intensity of the nucleic, cytoplasmic, and membrane staining (no staining = 0, weak staining = 1, moderate staining = 2, strong staining = 3) and the extent of stained cells (0–5% = 0, 5–25% = 1, 26–50% = 2, 51–75% = 3, 76–100% = 4). The final immunoreactive score was determined by multiplying the intensity score by the extent score of stained cells, ranging from 0 (the minimum score) to 12 (the maximum score).

Statistical Analysis—Statistical comparisons between only two groups were carried out by Student's *t* test or the Mann-Whitney rank sum test when a normal distribution could not be assumed. One-way analysis of variance followed by Dennett's post hoc test was used for multiple-group comparisons. Statistical calculations were carried out using SPSS version 19.0. We tested data for normality and variance and considered a p value of less than 0.05 significant.

RESULTS

An IP/MS Approach to Efficiently Identify Interactors of NEDL2—In a detailed study of the NEDL2 protein complex network, the IP protocol for protein complex isolation was performed. To maximize the number of protein identifications, we solved the immunocomplexes on SDS-PAGE and split each gel lane into three regions for subsequent sequencing in separate mass spectrometry runs. Interacting proteins of NEDL2 in HEK293T cells identified by mass spectrometry in two experiments are shown in supplemental Tables S1 and S2. High confidence interactions identified in one IP/MS experiment were chosen to compare with another experiment. We concluded that potential proteins that could interact with NEDL2 were highly enriched with mitotic proteins (Table 1). Except for several cell cycle-related proteins, including PRC1, NUSAP1, PLK1, CENPF, CEP170, and CLASP2, there was an interesting list of APC/C proteins. ANAPC1, ANAPC2, CDC27, ANAPC4, ANAPC5, CDC16, ANAPC7, CDC23, and Cdh1 were included in the list. The first eight proteins are all subunits of APC/C, and Cdh1 directly binds to and activates the APC/C ligase. Cdh1 maintains the activity of APC/C from late anaphase through G_1 phase, targeting cyclin B, Cdc20, and PLK1 for degradation. These results led us to examine whether the NEDL2 protein was involved in mitotic regulation.

NEDL2 Associates with Cdh1 in Vivo and in Vitro—We further confirmed the interaction of Cdh1 with NEDL2 in mammalian cells. Endogenous Cdh1 was co-immunoprecipitated with endogenous NEDL2, but not control IgG, from HeLa cells (Fig. 1*A*). To map the Cdh1-interacting region in NEDL2, a series of NEDL2 deletion mutants were generated (Fig. 1*B*). A co-IP assay was performed, and the result revealed that the C2 domain and the linker between the C2 and WW domain but not the WW domain and HECT domain of NEDL2 were required for Cdh1 binding (Fig. 1*C*). Additionally, a GST pull-down assay showed similar results (*i.e.* the N-terminal part of NEDL2

FIGURE 2. **NEDL2 is a substrate of APC/C-Cdh1 and one D-box is involved in NEDL2 degradation.** *A*, HEK293T cells were transfected with FLAG-NEDL2 and together with increasing amounts of HA-Cdh1. Cells were harvested 36 h later and analyzed by Western blotting. *B*, HEK293T cells were transfected with HA-Cdh1 and together with increasing amounts of FLAG-WT-NEDL2 and FLAG-C1540A-NEDL2. Cells were harvested 36 h later and analyzed by Western blotting. *C* and *D*, Cdh1 depletion increased the endogenous NEDL2 protein level but had no effect on NEDL2 mRNA level. HeLa cells were transfected with non-targeted control or Cdh1-specific siRNA, and the endogenous NEDL2 and Cdh1 levels were analyzed by immunoblot or real-time PCR. Data are presented as mean ± S.D. (*error bars*) (n = 3). *E* and *F*, NEDL2 depletion had no effect on endogenous Cdh1 protein and mRNA level. HeLa cells were transfected with non-targeted control or NEDL2-specific siRNA, and the endogenous NEDL2 and Cdh1 level were analyzed by immunoblot or real-time PCR. Data are presented as mean ± S.D. (n = 3). *G*, schematic representation of the Cdh1 protein functional domains. *H*, immunoblot analysis of whole cell lysates derived from HEK293T cells transfected with FLAG-NEDL2 together with the indicated Myc-Cdh1 constructs. *I*, immunoblot analysis of whole cell lysates derived from HeLa cells transfected with the indicated Myc-Cdh1 constructs. *J*, HEK293T cells were transfected with plasmids expressing either wild-type NEDL2 or mutants of NEDL2 together with or without a plasmid encoding HA-tagged wild-type Cdh1. *K*, HEK293T cells were transfected with NEDL2 mutants together with increasing amounts of HA-Cdh1. Cells were harvested 36 h later and analyzed by Western blotting. *L*, alignment of destruction box sequences in human, mouse, and rat NEDL2. *M*, HEK293T cells were transfected with plasmids expressing either NEDL2 324–1021 or NEDL2 324–1021-ΔRGSL together with or without HA-Cdh1. *N*, the experiments were similar to those in *M*, except the NEDL2 WT and ΔRGSL mutant were the full-length constructs. For *A*, *B*, *H*, *J*, *K*, *M*, and *N*, the GFP expression vector was included in each transfection as the transfection efficiency control.

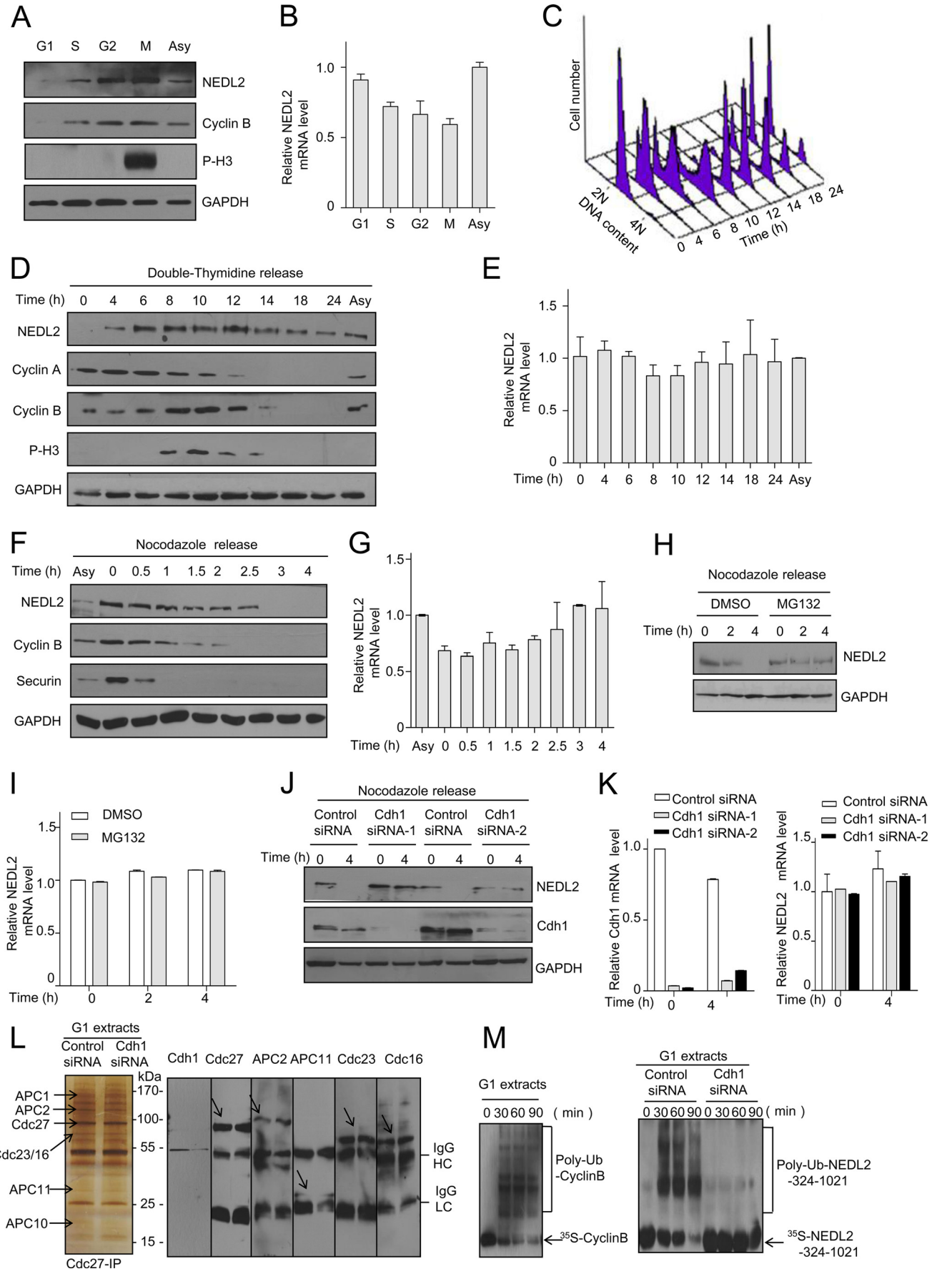
A
G1 S G2 M Asy
NEDL2
Cyclin B
P-H3
GAPDH
B
Relative NEDL2 mRNA level
1.0
0.5
0
G1 S G2 M Asy
C
Cell number
2N
4N
DNA content
0 4 6 8 10 12 14 18 24
Time (h)
D
Double-Thymidine release
Time (h) 0 4 6 8 10 12 14 18 24 Asy
NEDL2
Cyclin A
Cyclin B
P-H3
GAPDH
E
Relative NEDL2 mRNA level
1.5
1.0
0.5
0
Time (h) 0 4 6 8 10 12 14 18 24 Asy
F
Nocodazole release
Time (h) Asy 0 0.5 1 1.5 2 2.5 3 4
NEDL2
Cyclin B
Securin
GAPDH
G
Relative NEDL2 mRNA level
1.5
1.0
0.5
0
Time (h) Asy 0 0.5 1 1.5 2 2.5 3 4
H
Nocodazole release
DMSO MG132
Time (h) 0 2 4 0 2 4
NEDL2
GAPDH
I
DMSO
MG132
Relative NEDL2 mRNA level
1.5
1.0
0.5
0
Time (h) 0 2 4
J
Nocodazole release
Control siRNA
Cdh1 siRNA-1
Control siRNA
Cdh1 siRNA-2
Time (h) 0 4 0 4 0 4 0 4
NEDL2
Cdh1
GAPDH
K
Control siRNA
Cdh1 siRNA-1
Cdh1 siRNA-2
Relative Cdh1 mRNA level
1.0
0.5
0
Time (h) 0 4
Control siRNA
Cdh1 siRNA-1
Cdh1 siRNA-2
Relative NEDL2 mRNA level
1.5
1.0
0.5
0
Time (h) 0 4
L
G1 extracts
Control siRNA
Cdh1 siRNA
kDa
170-
100-
55 -
25 -
15 -
APC1
APC2
Cdc27
Cdc23/16
APC11
APC10
Cdc27-IP
Cdh1 Cdc27 APC2 APC11 Cdc23 Cdc16
IgG HC
IgG LC
M
G1 extracts
0 30 60 90 (min)
Poly-Ub -CyclinB
35S-CyclinB
G1 extracts
Control siRNA
Cdh1 siRNA
0 30 60 90 0 30 60 90 (min)
Poly-Ub-NEDL2 -324-1021
35S-NEDL2 -324-1021

mediated the interaction with Cdh1) (Fig. 1*D*). These results suggest that NEDL2 interacts with Cdh1 both *in vivo* and *in vitro*.

NEDL2 Is a Substrate of APC/C-Cdh1—Because APC/C and NEDL2 are both ubiquitin ligases, it is essential to investigate whether NEDL2 is a substrate of APC/C-Cdh1 or a ubiquitin ligase of Cdh1. Sequence analysis showed that NEDL2 contains a total of 11 putative D-boxes of the type R*XX*L (Fig. 1*B*), which might be recognized by APC/C-Cdh1. Therefore, we first examined the degradation of NEDL2 following ectopic overexpression of Cdh1 in HEK293T cells. The overexpression of Cdh1 resulted in a significant reduction in the protein level of WT-NEDL2 and ligase-defective C1540A-NEDL2 (Fig. 2*A*). It indicated that Cdh1 could mediate NEDL2 destruction independent of the ubiquitin ligase activity of NEDL2. By contrast, overexpression of NEDL2 could not induce the down-regulation of Cdh1 (Fig. 2*B*), suggesting that Cdh1 is not the substrate of NEDL2. To verify whether endogenous Cdh1 plays a role in controlling the NEDL2 level, Cdh1 was depleted by two independent siRNAs, and the mRNA and protein levels of NEDL2 were examined. Knockdown of Cdh1 increased the protein level but not the mRNA level of NEDL2 *in vivo* (Fig. 2, *C* and *D*). Conversely, knockdown of endogenous NEDL2 had no significant effects on Cdh1 levels (Figs. 2, *E* and *F*). Additionally, the degradation of NEDL2 could not be promoted by ectopic expression of ΔC-box-Cdh1 (Fig. 2, *G* and *H*), which is ubiquitin ligase activity-deficient due to its impaired ability to interact with the APC/C core complex. The result was similar to other well characterized Cdh1 substrates, such as cyclin B (Fig. 2*I*), indicating that Cdh1-mediated NEDL2 destruction depends on APC/C. These data suggest that NEDL2 is a substrate for APC/C-Cdh1.

Degradation of NEDL2 by APC/C-Cdh1 Is Dependent on Its RGSL Sequence—To identify which D-box(es) is responsible for the recognition and degradation by Cdh1, different NEDL2 deletion mutants were expressed in HEK293T cells with HA-Cdh1. Degradation analysis clearly showed that the N-terminal mutant 1–324 containing the first three D-boxes and the C-terminal 807–1572 containing the last seven D-boxes could not be degraded by overexpressed Cdh1 (Fig. 2*J*). By contrast, the middle region 324–1021 was efficiently degraded by Cdh1 (Fig. 2, *J* and *K*), suggesting that the 324–807 region contains the critical degradation signal. Within this region, only one D-box exists (*i.e.* the fourth D-box $R^{740}GSL^{743}$. This D-box is conserved among humans, mice, and rats (Fig. 2*L*). Deletion of this D-box (residues 740–743) in NEDL2 resulted in the resistance against Cdh1-mediated degradation (Fig. 2, *M* and *N*). These data strongly indicate that $R^{740}GSL^{743}$ is the *bona fide* degradation box of NEDL2 recognized by Cdh1.

NEDL2 Protein Level Reaches a Maximum in Mitosis and Is Degraded by APC/C-Cdh1 during Mitotic Exit—The APC/C-Cdh1 has a well established role in cell cycle control. To investigate the regulation of NEDL2 *in vivo*, we analyzed the protein levels of NEDL2 in G_1, S, G_2, and M phase. NEDL2 protein level was low in G_1 phase and reached a maximum in mitosis (Fig. 3*A*). Next, NEDL2 protein was tested across the cell cycle. HeLa cells were synchronized by a double-thymidine protocol, and the cell cycle profile of released cells was analyzed by flow cytometry (Fig. 3*C*). Western blot analysis showed that NEDL2 started to increase when cells entered S phase, and the expression was higher at 8–12 h after release, which was the peak of cyclin B expression during mitosis, and then dropped between the mitosis and G_1 phases (Fig. 3*D*). In order to ensure detailed kinetics of down-regulated NEDL2, cells were synchronized in M phase and then released from a thymidine/nocodazole block, and we observed that NEDL2 protein rapidly declined during the first 4 h after release as cells exited from mitosis and entered into G_1 phase (Fig. 3*F*). On the other hand, NEDL2 disappearance was preceded by that of cyclin B (Fig. 3, *D* and *F*), the degradation of which was initiated during the transition from metaphase to anaphase, suggesting that the regulation of NEDL2 occurred during late mitosis and early G_1 phases. The absence of NEDL2 could be explained by a down-regulation of NEDL2 transcription or a specific degradation of NEDL2 in G_1 phase, so we investigated the mRNA levels of NEDL2 in the same samples harvested in Fig. 3, *A*, *D*, and *F*. As shown in Fig. 3, *B*, *E*, and *G*, NEDL2 mRNA was present throughout the cell cycle, and there was no correlation between NEDL2 protein and mRNA levels in the cell cycle. These results suggest that the low NEDL2 protein level in G_1 phase results from protein degradation.

In order to investigate the mechanism of NEDL2 degradation, HeLa cells released from nocodazole into fresh medium were treated with the proteasome inhibitor MG132 for 4 h. MG132 treatment efficiently blocked the degradation of NEDL2 during mitotic exit independent of its mRNA abundance (Fig. 3, *H* and *I*), which revealed that NEDL2 was degraded by the proteasome. To confirm that the APC/C-Cdh1 is required for the destruction of NEDL2 during mitotic exit, Cdh1 was depleted by RNA interference. HeLa cells were transfected with two independent Cdh1-specific siRNAs or a control siRNA. NEDL2 protein remained at a high level 4 h postrelease

FIGURE 3. **NEDL2 is ubiquitinated and degraded by APC/C-Cdh1 during mitotic exit.** *A*, analysis of NEDL2 protein levels in HeLa cells, which were synchronized at the indicated cell cycle phases. *B*, the samples harvested in *A* were analyzed by real-time PCR. Data are presented as mean ± S.D. (*error bars*) ($n = 3$). *C*, HeLa cells were synchronized at S phase by double-thymidine block. At the indicated hours after release from the block, cell lysates were collected and analyzed for DNA content by flow cytometry. *D*, the same samples harvested in *C* were analyzed by immunoblotting for the proteins as shown. *E*, the samples harvested in *D* were analyzed by real-time PCR. Data are presented as mean ± S.D. ($n = 3$). *F*, HeLa cells were synchronized at prometaphase by thymidine-nocodazole and then released for the indicated times. Cell lysates were detected with antibodies against NEDL2, cyclin B, and securin. *G*, the samples harvested in *F* were analyzed by real-time PCR. Data are presented as mean ± S.D. ($n = 3$). *H*, nocodazole-arrested mitotic HeLa cells were released into fresh medium containing DMSO or 20 μM MG132 for different times and analyzed by Western blot. *I*, the samples harvested in *H* were analyzed by real-time PCR. Data are presented as mean ± S.D. ($n = 3$). *J*, HeLa cells transfected with control or Cdh1 siRNA were arrested at mitosis by nocodazole treatment (0 h) and released into fresh medium for 4 h, and then NEDL2 protein levels were detected. *K*, the samples harvested in *J* were analyzed by real-time PCR. Data are presented as mean ± S.D. ($n = 3$). *L*, immunopurified G_1 phase APC/C was separated by SDS-PAGE and analyzed by silver staining and immunoblotting with Cdc27, APC2, APC11, Cdc23, and Cdc16 antibodies. *M*, *in vitro* ubiquitination assays were carried out with *in vitro*-translated ^{35}S-labeled NEDL2 324–1021 mutant using the complete or Cdh1-depleted extracts for the time indicated. Cyclin B was used as a positive control substrate. The reaction products were analyzed by SDS-PAGE prior to autoradiography.

in cells transfected with Cdh1 siRNA. By contrast, NEDL2 levels decreased substantially 4 h postrelease in cells transfected with control siRNA (Fig. 3*J*). Likewise, the regulation was not due to the change of NEDL2 mRNA abundance (Fig. 3*K*).

Next we performed *in vitro* ubiquitination assays to directly show that APC/C-Cdh1 is the E3 ligase of NEDL2. APC/C was purified by immunoprecipitation with a Cdc27 antibody from G_1 phase extracts, which were derived from HeLa cells transfected with control siRNA or Cdh1 siRNA. Silver-stained SDS-PAGE showed a comparison of purified APC/C (Fig. 3*L*). Cdc27 immunoprecipitates were also assayed by immunoblotting to determine the depletion of Cdh1 and the presence of Cdc27, the APC/C catalytic core subunits APC2 and APC11, and the tetratricopeptide repeat domain-containing subunits Cdc16 and Cdc23 (Fig. 3*L*). We then carried out *in vitro* ubiquitination assays using the purified APC/C and Cdh1 complex with ^{35}S-labeled NEDL2 or cyclin B. As shown in Fig. 3*M*, *in vitro* translated cyclin B was efficiently ubiquitinated by APC/C, indicating that the purified APC/C complex harbors ubiquitin ligase activity. Then we examined the NEDL2 ubiquitination by APC/C. The results showed that NEDL2 324–1021 was efficiently ubiquitinated *in vitro* as early as at 30 min of incubation, and the ubiquitination was detectable throughout the 90-min course. This process was dependent on the presence of Cdh1 because the depletion of Cdh1 significantly attenuated the ubiquitination of NEDL2 (Fig. 3*M*, *right*). Taken together, these results demonstrate that NEDL2 protein level is cell cycle-regulated, and it is a novel substrate of the APC/C-Cdh1 complex by which it is targeted to proteasome-dependent degradation during mitotic exit.

NEDL2 Localizes on the Mitotic Spindles throughout Mitosis—The expression pattern of NEDL2 suggests that it may play a role during mitosis. To address this issue, we examined the subcellular localization of NEDL2, which ensured the absence of NEDL2 in G_1 phase. NEDL2 colocalized with a microtubule marker, α-tubulin in S and G_2 phase and mainly localized at mitotic spindles during mitosis (Fig. 4*A*). In untreated HeLa cells, NEDL2 and α-tubulin were arranged into a circular pattern around the nucleus. After a 4-h incubation in 100 ng/ml nocodazole, an MT depolymerization drug, both α-tubulin and NEDL2 were dispersed (Fig. 4*B*), indicating that NEDL2 was directly associated with the mitotic spindle. NEDL2, a new spindle-associated protein, may be involved in the organization and regulation of mitotic spindles during the M phases, and it is degraded during mitotic exit. However, it has not been studied in such fields.

Depletion of NEDL2 Causes a Marked Delay in the Onset of Anaphase—To investigate the function of NEDL2 in mitosis, we examined the effects of siRNA-mediated NEDL2 depletion on divisions of HeLa cells. Flow cytometry demonstrated that 24% of control cells were arrested with 4N DNA content 14 h after release from the thymidine block, whereas about 40% of NEDL2-depleted cells had 4N DNA (Fig. 5*A*). It suggested that NEDL2 silencing inhibited mitotic progression. We next monitored mitotic progression by time-lapse imaging of HeLa cells stably expressing green fluorescent protein (GFP)-tagged histone H2B. We found that NEDL2 knockdown caused a marked delay in the onset of anaphase, compared with the control

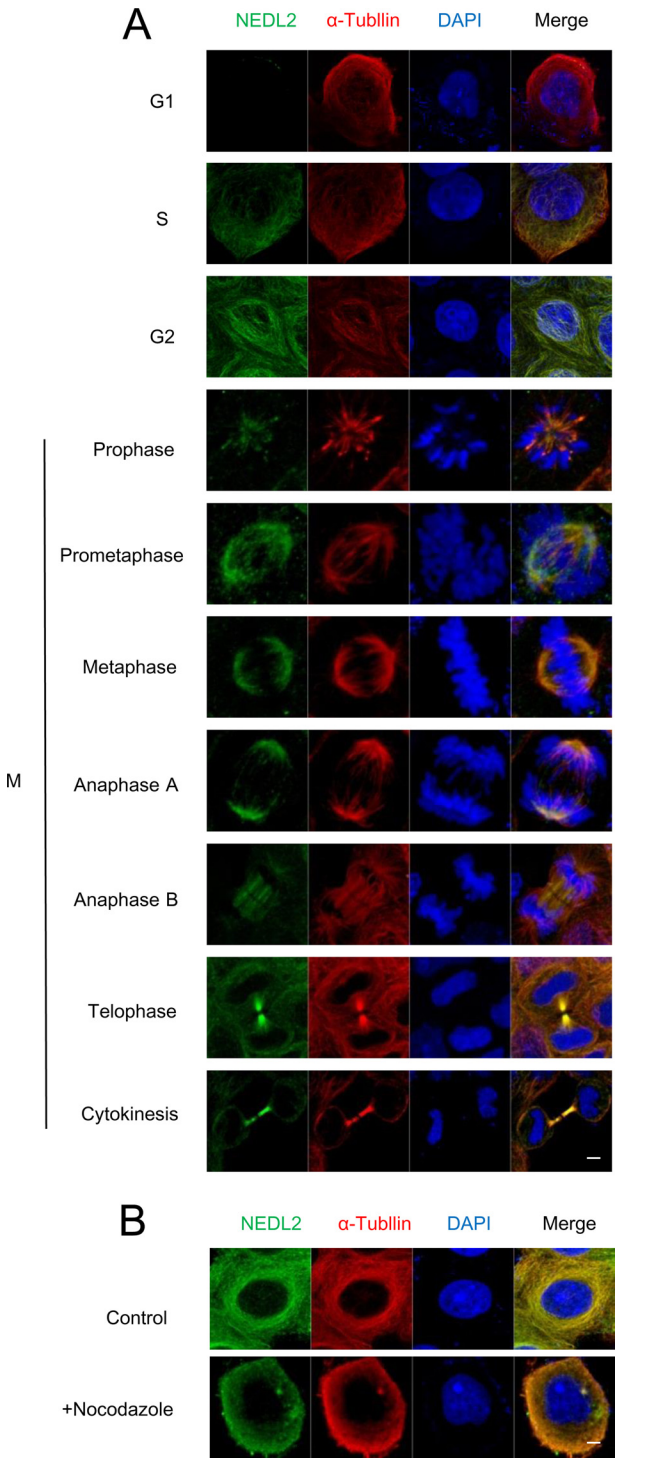

FIGURE 4. **NEDL2 is a spindle-associated protein.** *A*, immunofluorescent stainings were carried out to check NEDL2 localization changes during different cell cycle phases. *Scale bar*, 10 μm. *B*, HeLa cells were incubated in 100 ng/ml nocodazole or DMSO. Immunofluorescent stainings were carried out to check NEDL2 and α-tubulin. *Scale bar*, 10 μm.

siRNA (Fig. 5*B* and supplemental Movies S1 and S2). The average duration in mitosis increased from 56 min in control siRNA cells ($n = 137$) to 96 min in NEDL2 knockdown cells ($n = 137$; Fig. 5*C*). Interestingly, the NEDL2 knockdown-induced delay of anaphase onset was due to a significant elongation of metaphase, although the duration of prometaphase was almost

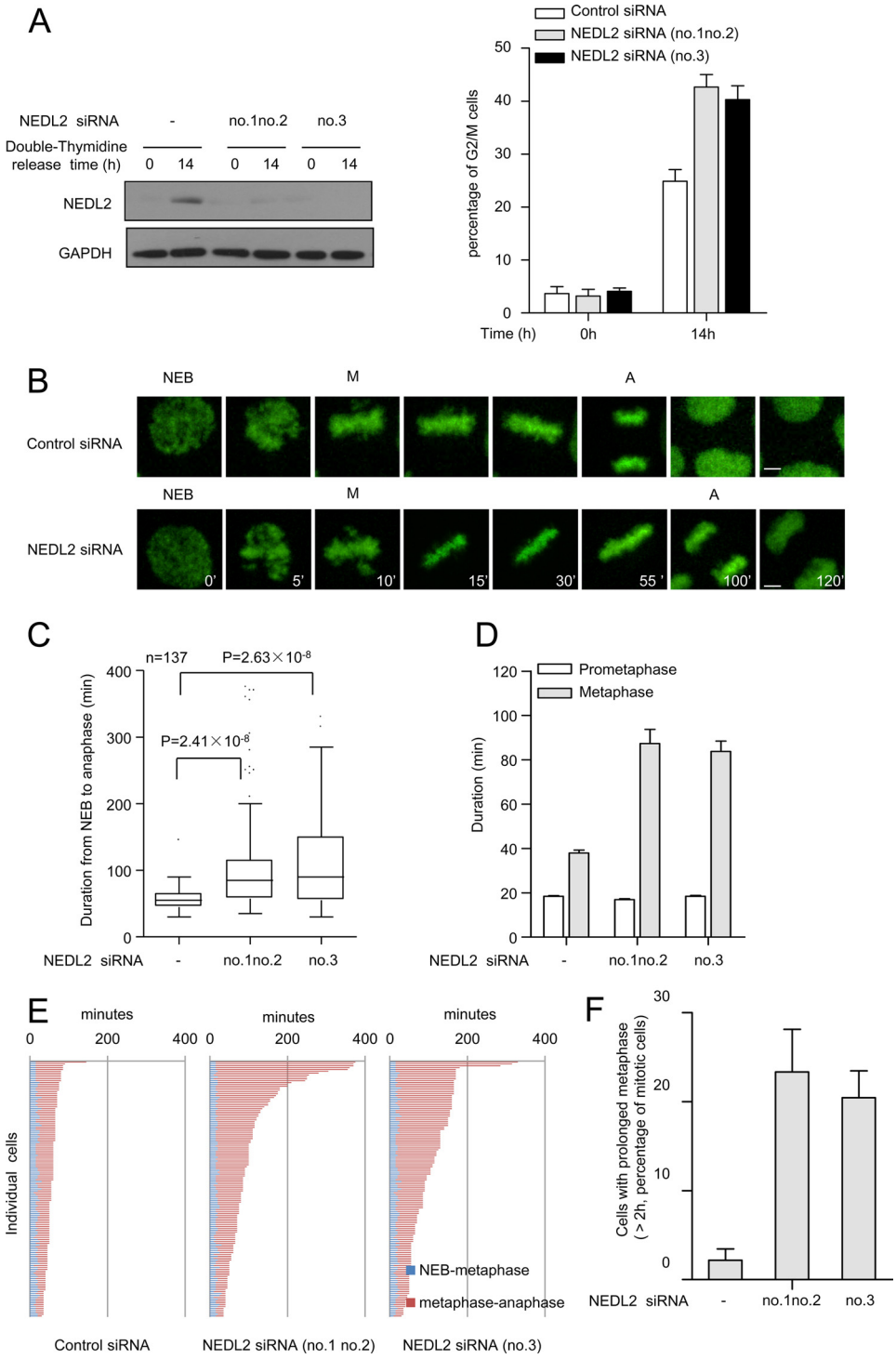

FIGURE 5. **NEDL2 knockdown induces delay of anaphase onset.** *A*, HeLa cells transfected with control siRNA or NEDL2 siRNA were synchronized by a double thymidine and then fixed at the indicated times and subject to flow cytometry (*right*). NEDL2 protein level in the samples was determined by immunoblotting (*left*). *B*, NEDL2 siRNA-transfected cells exhibit a marked delay of anaphase onset. Selected frames from time lapse movies of representative HeLa/GFP-H2B cells transfected with control, NEDL2 siRNA. The time on the images is in minutes. *NEB*, nuclear envelope breakdown; *M*, metaphase; *A*, anaphase. *Scale bar*, 5 μm. *C*, a *box-and-whisker plot* showing the duration from nuclear envelope breakdown to anaphase onset in HeLa/GFP-H2B cells with NEDL2 knockdown ($n = 137$ cells) or control knockdown ($n = 137$ cells). *D*, the lengths of prometaphase and metaphase in control ($n = 137$ cells) and NEDL2 knockdown cells ($n = 137$ cells) were analyzed. Data are shown as mean ± S.E. (*error bars*). *E*, graph of the cumulative duration of mitotic phases in the cells described in *B*. Each *bar* represents one cell. *Bars* indicate the time from nuclear envelope breakdown to metaphase (*blue*) and the time from the first frame of metaphase to anaphase onset (*red*). *F*, the percentage of cells taking longer than 2 h for the duration of metaphase in the cells transfected with NEDL2 siRNA. Data are shown as mean ± S.E. and are representative of three independent experiments.

unchanged (Fig. 5, *D* and *E*). Data also showed that about 22% NEDL2-depleted cells took 2 h longer for the duration of metaphase, compared with the cells transfected with control siRNA (Fig. 5*F*). Taken together, different from another HECT type ubiquitin ligase Smurf2, depletion of which leads to increased misalignment and missegregation of chromosomes, premature

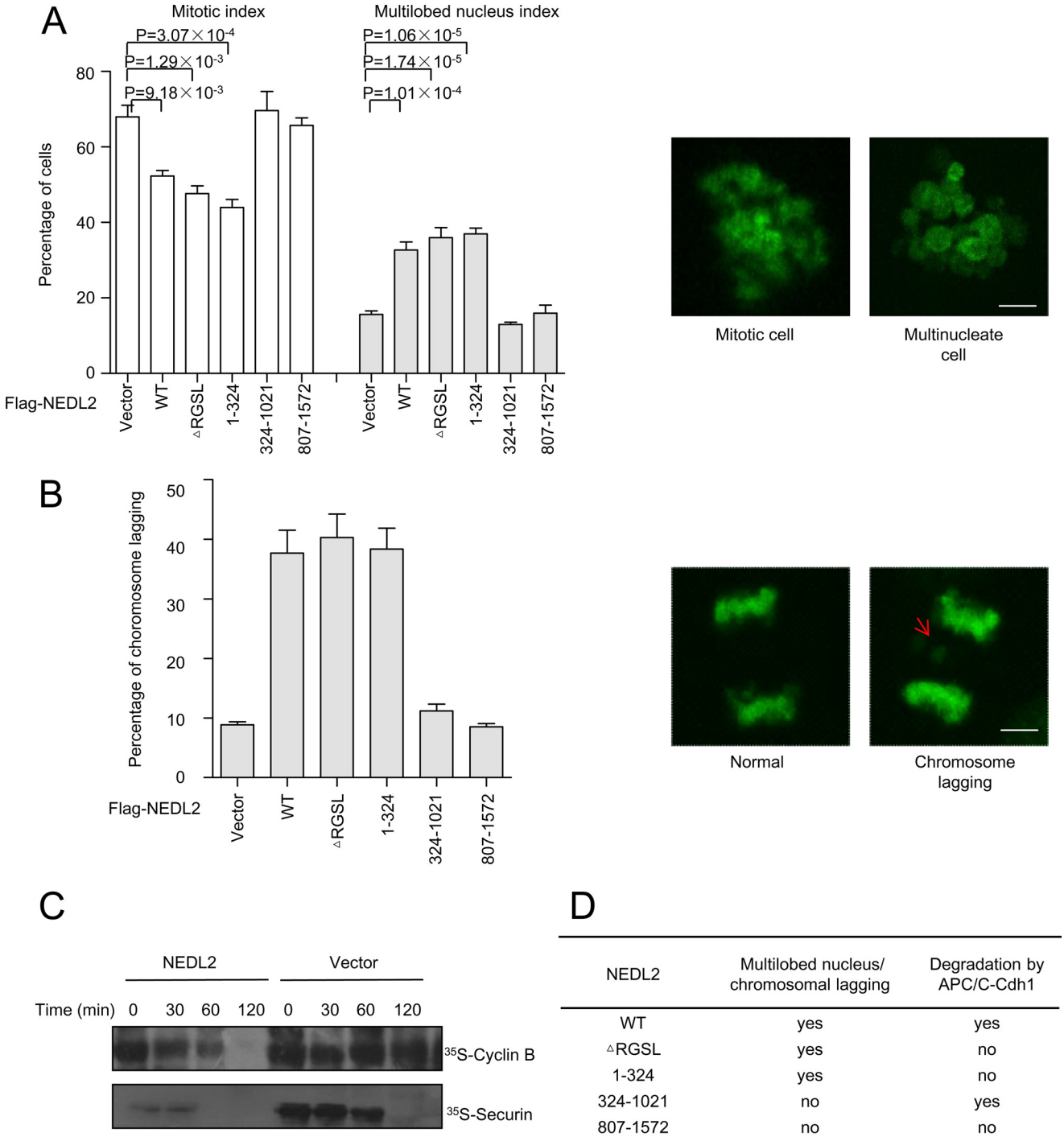

NEDL2	Multilobed nucleus/ chromosomal lagging	Degradation by APC/C-Cdh1
WT	yes	yes
△RGSL	yes	no
1-324	yes	no
324-1021	no	yes
807-1572	no	no

FIGURE 6. **Overexpression of NEDL2 leads to chromosome missegregation.** *A*, HeLa/GFP-H2B cells overexpressed with NEDL2 or its mutants were treated with taxol. After 24 h, the mitotic index and multilobed nucleus index were determined. Data are representative of three independent experiments. *Error bars*, S.E. Representative images of mitotic cell and polykaryocytes are shown (*right*). *Scale bar*, 5 μm. *B*, analysis of chromosome segregation defects in HeLa cells expressing NEDL2 or its mutants. Data are representative of three independent experiments. *Error bars*, S.E. Representative images of normal and lagging chromosomes in HeLa cells are shown (*right*). *Scale bar*, 5 μm. *C*, *in vitro* degradation assays. Control or NEDL2-overexpressed extracts from nocodazole-arrested HeLa cells were supplemented with an energy-regenerating system, and reactions were initiated by the addition of ^{35}S-labeled cyclin B or securin proteins. Samples were then taken at the indicated times and analyzed by SDS-PAGE and autoradiography. *D*, summary of the possibility of chromosome lagging and the stability of the NEDL2 mutants. The stability of the mutants was determined as described above.

anaphase onset (16), NEDL2 silencing inhibits metaphase-anaphase transition.

Overexpression of NEDL2 Induces Chromosomal Lagging—To further determine the potential role of NEDL2 in metaphase-anaphase transition, we tested whether overexpression of NEDL2 could override taxol-induced mitotic arrest. Compared with empty vector, the percentage of mitotic cells was much lower in NEDL2-expressing cells after taxol treatment, but the percentage of cells with multilobed nuclei was higher (Fig. 6*A*). The result indicated that overexpression of NEDL2 may lead to earlier APC/C activation. We then found that the percentage of cells with lagging chromosomes, an important

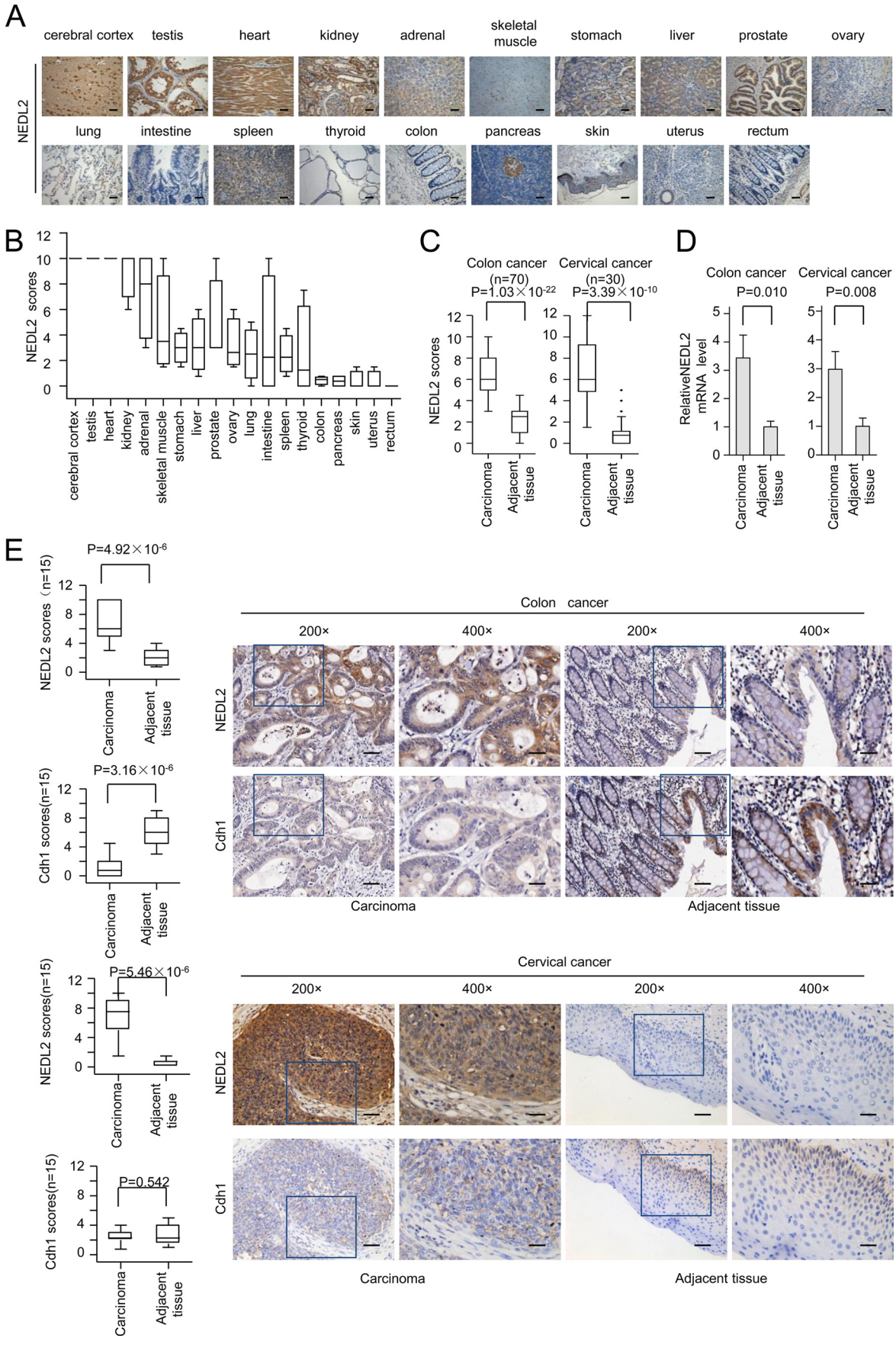
A
cerebral cortex
testis
heart
kidney
adrenal
skeletal muscle
stomach
liver
prostate
ovary
NEDL2
lung
intestine
spleen
thyroid
colon
pancreas
skin
uterus
rectum
B
NEDL2 scores
C
Colon cancer (n=70) P=1.03×10-22
Cervical cancer (n=30) P=3.39×10-10
NEDL2 scores
Carcinoma
Adjacent tissue
D
Colon cancer P=0.010
Cervical cancer P=0.008
RelativeNEDL2 mRNA level
E
P=4.92×10-6
NEDL2 scores（n=15）
P=3.16×10-6
Cdh1 scores(n=15)
P=5.46×10-6
NEDL2 scores(n=15)
P=0.542
Cdh1 scores(n=15)
Colon cancer
200×
400×
NEDL2
Cdh1
Carcinoma
Adjacent tissue
Cervical cancer

index of chromosomal instability that might result from premature APC/C activation, increased in NEDL2-expressing cells (Fig. 6*B*). Next, we used the cell-free system to test the effects of NEDL2 on APC/C activity. The degradation of cyclin B and securin was markedly advanced in NEDL2 overexpression extracts (Fig. 6*C*), which directly verified that NEDL2 was required for the APC/C activation.

We also investigated whether the APC/C-Cdh1-regulated NEDL2 stability was implicated in mitotic progression. NEDL2-ΔRGSL and N-terminal 1–324 mutant (containing the C2 domain) behaved similarly to wild-type NEDL2. By contrast, 324–1021 and 807–1572 mutants could not override taxol-induced mitotic arrest (Fig. 6*A*). A similar conclusion was made in the chromosomal lagging assays (Fig. 6*B*). Because NEDL2-ΔRGSL, 1–324 and 807–1572 mutants were not degraded by Cdh1 (Fig. 2, *J*, *M*, and *N*), the recognition by Cdh1 seems not to be tightly related to the ability of NEDL2 to regulate cell cycle progression (Fig. 6*D*).

NEDL2 Protein Level Is Elevated in Several Types of Human Tumors—The majority of cancers involve chromosomal instability (17). Deregulation of cyclins and other cell cycle regulators can cause genomic instability, and aberrant expression of cell cycle regulators can be detected in various malignant tumors (18). Because overexpression of NEDL2 enhances chromosomal instability, it may induce the human tumors. We first screened the expression spectrum of NEDL2 in various tissues by immunohistochemistry staining. Consistent with the previous report that NEDL2 mRNA expresses predominantly in the adult brain, heart, and lung (14), NEDL2 protein was highly expressed in cerebral cortex, testis, heart, kidney, and adrenal but was weakly detected in colon, pancreas, skin, uterus, and rectum (Fig. 7, *A* and *B*).

Next, we screened several types of tumors, of which their normal tissues expressed little NEDL2, including colon cancer, rectal cancer, cervix cancer, pancreas cancer, lung cancer, and liver cancer. The results showed that expression of NEDL2 protein was significantly up-regulated in colon and cervix tumor tissues, compared with matched adjacent normal tissues (Fig. 7, *C* and *E*). Moreover, mRNA levels of NEDL2 in colon and cervix tumor tissues were significantly higher than those in matched adjacent normal tissues (Fig. 7*D*). A higher frequency of positive NEDL2 expression was observed in colon cancer tissue, whereas a lower frequency of Cdh1 expression was measured in the cancer area (Fig. 7*E*). Thus, NEDL2 and Cdh1 were inversely correlated in colon cancer. However, Cdh1 was expressed at comparable levels between the cervical cancer and the adjacent tissues. Similar expression profilings of Cdh1 have been reported in a previous study (19). Taken together, we propose that both the increase of mRNA synthesis and the decrease of protein degradation by Cdh1 might contribute to the elevated expression of NEDL2 in cancer tissues, at least in the colon cancer. This study is the first evidence to establish the relationship between the NEDL2 protein and tumors.

DISCUSSION

Protein-protein interactions constitute the molecular backbone of cell biology, where select proteins assemble into metastable complexes to form bioactive units (20, 21). IP/MS has recently emerged as a preferred method in the analysis of protein complex components and cellular protein networks (22). In the case of NEDL2, a HECT type ubiquitin ligase stabilizing p73 and degrading ATR kinase, we performed an unbiased study of its protein complex networks. We analyzed the functional specificity of candidate proteins after using IP/MS, and fortunately this strategy has proved to be extremely successful. A list of mitotic proteins were identified by IP/MS, and the following evidence indicated that NEDL2 was indeed a regulator of mitosis and was degraded by APC/C-Cdh1, which was identified in the approach described above. On the other hand, NEDL2 was demonstrated to localize on mitotic spindles in the study. Microtubule-associated proteins and kinesins could also be found in the candidate proteins. Certainly, many other high confidence interactions are worthy of further study. Indeed, this is a generally applicable approach to identify protein complex networks important for many biological processes.

The APC/C E3 ubiquitin ligase consists of at least 13 proteins. The RING finger protein, APC11, and the Cul1-related scaffold protein, APC2, form the catalytic core of the complex (23). APC substrate specificity is conferred by recruitment of a co-activator protein, Cdh1 or Cdc20. Both Cdh1 and Cdc20 target specific proteins for ubiquitination through the recognition of substrates containing a destruction box, or D-box, whereas Cdh1 recruits additional substrates containing other targeting motifs, including the KEN box, A-box, and CRY box (24, 25). Although NEDL2 contains 11 D-boxes, Cdh1 can specifically recognize only one of its D-boxes, which is located at amino acids 740–743 (RGSL) for degradation.

Cdh1 can also function in an APC complex-free mode. Recent exciting evidence has uncovered unexpected neurobiological, myogenesis, or other functions for Cdh1 (26–28). Another member of the Nedd4 family, Smad ubiquitination regulatory factor 1 (Smurf1), can be degraded by Cdh1 in its regulation of osteoblast function and axon growth in an APC/C-independent or -dependent manner, respectively (29, 30). NEDL2, whose mRNA was preferentially expressed in neuronal tissue, as previously reported (14), may function along with Cdh1 in regulation of neurobiological function or other physiological processes besides in cell cycle control. Cdh1 can ubiquitinate NEDL2 and degrade it in mitotic exit. Cdh1 deregulation may result in the increased expression of NEDL2, which may induce the colon tumor. But their physiological functions

FIGURE 7. **The expression of NEDL2 is elevated in human tumor tissues.** *A*, images of immunohistochemical staining for NEDL2 in 19 types of tissues. *Scale bar*, 50 μm. *B*, *box plot* of NEDL2 expression in 19 kinds of tissues. *C*, the tissue array of colon and cervix cancer was carried out by immunohistochemistry with anti-NEDL2 antibody. *D*, quantitative RT-PCR analysis of NEDL2 mRNA level in colon and cervix cancer tissues and matched adjacent normal control from 15 subjects. Data were analyzed using Student's *t* test. Data are shown as means ± S.D. (*error bars*) of three independent experiments. *E*, NEDL2 and Cdh1 protein levels in colon and cervix cancer samples (*left*). Representative images of immunohistochemical staining for NEDL2 and Cdh1 are shown (*right*). *Scale bar*, 50 μm (×200) and 25 μm (×400).

are still needed to be fully understood in other cellular processes.

During metaphase-anaphase transition, APC/C mediates the ubiquitination of securin, mitotic cyclins, and other substrates for anaphase onset (31). The spindle assembly checkpoint (SAC) is a surveillance mechanism that ensures accurate chromosome segregation (32, 33). SAC is activated by improperly attached kinetochores and then inhibits the ability of APC/C to target the substrates for degradation to prevent anaphase onset until each kinetochore is stably bioriented on the spindle (34). Once the microtubule kinetochore attachment and tension are fully established, the SAC signals are turned off, and APC/C-Cdc20 is activated. Although it has been well established that SAC must be inactivated before anaphase onset, the molecular mechanisms of SAC inactivation remain obscure. NEDL2 is a novel regulator of anaphase onset. Inhibition of NEDL2 delays the metaphase to anaphase transition, whereas overexpression of NEDL2 leads to earlier release of APC/C and chromosome missegregation. Chromosome missegregation occurs when the SAC is defective and APC/C is prematurely activated. We speculated that NEDL2 might regulate SAC inactivation or the activation of APC/C.

It has been reported that dysregulation of SAC causes chromosome missegregation, chromosome instability, and aneuploidy (35, 36). It is clear that aneuploidy can promote tumorigenesis in certain contexts (37, 38). Ectopic expression of NEDL2 protein and mRNA was found in colon and cervix tumor tissues. It indicates that dysregulation of NEDL2 disturbs the metaphase to anaphase transition, which may lead to tumorigenesis. Consistent with NEDL2, the oncogenic potential of the Nedd4-like E3s is highlighted by the identification of a number of tumor suppressor molecules among their substrates. The assertion that Nedd4-like ubiquitin ligases play a role in cancer is supported by the overexpression of Smurf2 in esophageal squamous cell carcinoma, WWP1 in prostate and breast cancer, Nedd4 in prostate and bladder cancer, and Smurf1 in pancreatic cancer (10).

In conclusion, we found NEDL2 as a novel substrate of APC/C-Cdh1 during mitotic exit, and depletion of Cdh1 leads to significantly elevated levels of NEDL2, which may cause the colon cancer. It will be interesting to further investigate the physiological significance of the degradation of NEDL2 in cell cycle regulation or other physiological processes. This is the first time that the role of NEDL2 in the regulation of metaphase to anaphase transition has been shown, and it is worth investigating whether NEDL2 promotes the metaphase to anaphase transition by regulating SAC inactivation or the activation of APC/C. In addition, we uncovered the abnormal overexpression NEDL2 in human tumors, and it will be important to study the relationship between the imbalance of NEDL2 in mitotic progression and tumorigenesis.

Acknowledgments—We thank Drs. Xue-Min Zhang, Hui-Yan Li, Teng Li, and Yan Chang for important suggestions and for providing materials.

REFERENCES

1. Pickart, C. M. (2001) Mechanisms underlying ubiquitination. *Annu. Rev. Biochem.* **70,** 503–533
2. Peters, J. M. (2006) The anaphase promoting complex/cyclosome. A machine designed to destroy. *Nat. Rev. Mol. Cell Biol.* **7,** 644–656
3. Hagting, A., Den Elzen, N., Vodermaier, H. C., Waizenegger, I. C., Peters, J. M., and Pines, J. (2002) Human securin proteolysis is controlled by the spindle checkpoint and reveals when the APC/C switches from activation by Cdc20 to Cdh1. *J. Cell Biol.* **157,** 1125–1137
4. Schwab, M., Lutum, A. S., and Seufert, W. (1997) Yeast Hct1 is a regulator of Clb2 cyclin proteolysis. *Cell* **90,** 683–693
5. Visintin, R., Prinz, S., and Amon, A. (1997) CDC20 and CDH1. A family of substrate-specific activators of APC-dependent proteolysis. *Science* **278,** 460–463
6. Kramer, E. R., Gieffers, C., Hölzl, G., Hengstschläger, M., and Peters, J. M. (1998) Activation of the human anaphase-promoting complex by proteins of the CDC20/Fizzy family. *Curr. Biol.* **8,** 1207–1210
7. Fang, G., Yu, H., and Kirschner, M. W. (1998) Direct binding of CDC20 protein family members activates the anaphase-promoting complex in mitosis and G_1. *Mol. Cell* **2,** 163–171
8. Tang, Z., Bharadwaj, R., Li, B., and Yu, H. (2001) Mad2-independent inhibition of APCCdc20 by the mitotic checkpoint protein BubR1. *Dev. Cell* **1,** 227–237
9. Schwarz, S. E., Rosa, J. L., and Scheffner, M. (1998) Characterization of human hect domain family members and their interaction with UbcH5 and UbcH7. *J. Biol. Chem.* **273,** 12148–12154
10. Chen, C., and Matesic, L. E. (2007) The Nedd4-like family of E3 ubiquitin ligases and cancer. *Cancer Metastasis Rev.* **26,** 587–604
11. Miyazaki, K., Fujita, T., Ozaki, T., Kato, C., Kurose, Y., Sakamoto, M., Kato, S., Goto, T., Itoyama, Y., Aoki, M., and Nakagawara, A. (2004) NEDL1, a novel ubiquitin-protein isopeptide ligase for dishevelled-1, targets mutant superoxide dismutase-1. *J. Biol. Chem.* **279,** 11327–11335
12. Li, Y., Ozaki, T., Kikuchi, H., Yamamoto, H., Ohira, M., and Nakagawara, A. (2008) A novel HECT-type E3 ubiquitin protein ligase NEDL1 enhances the p53-mediated apoptotic cell death in its catalytic activity-independent manner. *Oncogene* **27,** 3700–3709
13. Zhang, L., Haraguchi, S., Koda, T., Hashimoto, K., and Nakagawara, A. (2011) Muscle atrophy and motor neuron degeneration in human NEDL1 transgenic mice. *J. Biomed. Biotechnol.* **2011,** 831092
14. Miyazaki, K., Ozaki, T., Kato, C., Hanamoto, T., Fujita, T., Irino, S., Watanabe, K., Nakagawa, T., and Nakagawara, A. (2003) A novel HECT-type E3 ubiquitin ligase, NEDL2, stabilizes p73 and enhances its transcriptional activity. *Biochem. Biophys. Res. Commun.* **308,** 106–113
15. Muralikrishna, B., Chaturvedi, P., Sinha, K., and Parnaik, V. K. (2012) Lamin misexpression upregulates three distinct ubiquitin ligase systems that degrade ATR kinase in HeLa cells. *Mol. Cell. Biochem.* **365,** 323–332
16. Osmundson, E. C., Ray, D., Moore, F. E., Gao, Q., Thomsen, G. H., and Kiyokawa, H. (2008) The HECT E3 ligase Smurf2 is required for Mad2-dependent spindle assembly checkpoint. *J. Cell Biol.* **183,** 267–277
17. Rajagopalan, H., Nowak, M. A., Vogelstein, B., and Lengauer, C. (2003) The significance of unstable chromosomes in colorectal cancer. *Nat. Rev. Cancer* **3,** 695–701
18. Wäsch, R., and Engelbert, D. (2005) Anaphase-promoting complex-dependent proteolysis of cell cycle regulators and genomic instability of cancer cells. *Oncogene* **24,** 1–10
19. Fujita, T., Liu, W., Doihara, H., and Wan, Y. (2008) Regulation of Skp2-p27 axis by the Cdh1/anaphase-promoting complex pathway in colorectal tumorigenesis. *Am. J. Pathol.* **173,** 217–228
20. Alberts, B. (1998) The cell as a collection of protein machines. Preparing the next generation of molecular biologists. *Cell* **92,** 291–294
21. Köcher, T., and Superti-Furga, G. (2007) Mass spectrometry-based functional proteomics. From molecular machines to protein networks. *Nat. Methods* **4,** 807–815
22. Malovannaya, A., Li, Y., Bulynko, Y., Jung, S. Y., Wang, Y., Lanz, R. B., O'Malley, B. W., and Qin, J. (2010) Streamlined analysis schema for high-throughput identification of endogenous protein complexes. *Proc. Natl.*

Acad. Sci. **107,** 2431–2436
23. Kim, A. H., and Bonni, A. (2007) Thinking within the D box. Initial identification of Cdh1-APC substrates in the nervous system. *Mol. Cell Neurosci.* **34,** 281–287
24. Reis, A., Levasseur, M., Chang, H. Y., Elliott, D. J., and Jones, K. T. (2006) The CRY box. A second APCcdh1-dependent degron in mammalian cdc20. *EMBO Rep.* **7,** 1040–1045
25. Littlepage, L. E., and Ruderman, J. V. (2002) Identification of a new APC/C recognition domain, the A box, which is required for the Cdh1-dependent destruction of the kinase Aurora-A during mitotic exit. *Genes Dev.* **16,** 2274–2285
26. Gieffers, C., Peters, B. H., Kramer, E. R., Dotti, C. G., and Peters, J. M. (1999) Expression of the CDH1-associated form of the anaphase-promoting complex in postmitotic neurons. *Proc. Natl. Acad. Sci. U.S.A.* **96,** 11317–11322
27. Konishi, Y., Stegmüller, J., Matsuda, T., Bonni, S., and Bonni, A. (2004) Cdh1-APC controls axonal growth and patterning in the mammalian brain. *Science* **303,** 1026–1030
28. Li, W., Wu, G., and Wan, Y. (2007) The dual effects of Cdh1/APC in myogenesis. *FASEB J.* **21,** 3606–3617
29. Kannan, M., Lee, S. J., Schwedhelm-Domeyer, N., and Stegmüller, J. (2012) The E3 ligase Cdh1-anaphase promoting complex operates upstream of the E3 ligase Smurf1 in the control of axon growth. *Development* **139,** 3600–3612
30. Kannan, M., Lee, S. J., Schwedhelm-Domeyer, N., Nakazawa, T., and Stegmüller, J. (2012) p250GAP is a novel player in the Cdh1-APC/Smurf1 pathway of axon growth regulation. *PLoS One* **7,** e50735
31. Yu, H. (2007) Cdc20. A WD40 activator for a cell cycle degradation machine. *Mol. Cell* **27,** 3–16
32. Bharadwaj, R., and Yu, H. (2004) The spindle checkpoint, aneuploidy, and cancer. *Oncogene* **23,** 2016–2027
33. Musacchio, A., and Salmon, E. D. (2007) The spindle-assembly checkpoint in space and time. *Nat. Rev. Mol. Cell Biol.* **8,** 379–393
34. Pesin, J. A., and Orr-Weaver, T. L. (2008) Regulation of APC/C activators in mitosis and meiosis. *Annu. Rev. Cell Dev. Biol.* **24,** 475–499
35. Michor, F. (2005) Chromosomal instability and human cancer. *Philos. Trans. R. Soc. Lond. B Biol. Sci.* **360,** 631–635
36. Lengauer, C., and Wang, Z. (2004) From spindle checkpoint to cancer. *Nat. Genet.* **36,** 1144–1145
37. Schvartzman, J. M., Sotillo, R., and Benezra, R. (2010) Mitotic chromosomal instability and cancer. Mouse modelling of the human disease. *Nat. Rev. Cancer* **10,** 102–115
38. Weaver, B. A., and Cleveland, D. W. (2008) The aneuploidy paradox in cell growth and tumorigenesis. *Cancer Cell* **14,** 431–433